ELSEVIER

Contents lists available at ScienceDirect

Composites Part A

journal homepage: www.elsevier.com/locate/compositesa





Insights into the effect of fiber–matrix interphase physiochemicalmechanical properties on delamination resistance and fracture toughness of hybrid composites

Hamed Fallahi ^{a,1}, Ozge Kaynan ^{b,1}, Amir Asadi ^{a,b,c,*}

- ^a J. Mike Walker '66 Department of Mechanical Engineering, Texas A&M University, College Station, TX 77843, United States
- ^b Department of Materials Science and Engineering, Texas A&M University, College Station, TX 77843-3367, United States
- ^c Department of Engineering Technology and Industrial Distribution, Texas A&M University, College Station, TX 77843-3367, United States

ARTICLE INFO

Keywords: Carbon fiber (A) Delamination (B) Fiber/matrix bond (B) Mechanical testing (D)

ABSTRACT

The characteristics of the formed fiber–matrix interphase play a decisive role during fracture of fiber reinforced composites. Herein, we experimentally investigate the influence of fiber–matrix interphase on the fracture toughness of fiber-reinforced composites. Carbon fiber is modified with nanoparticles having different physical and chemical features, including functionalized carbon nanotubes (fCNTs), cellulose nanocrystals (CNCs), and hybrid CNC-CNT, and the effect of chemical and mechanical properties of the fiber–matrix interphase and fiber surface topology on the mode I and mode II delamination resistance of carbon fiber/epoxy composites is studied. The objective of this study is to fundamentally understand the relationship of fiber–matrix interphase properties and fracture toughness. It is observed that fiber–matrix interfacial strength depends on the width and chemical properties of the interphase zone. CNC-CNT spans the interfacial zone enhancing the interfacial strength by 76%, allowing the matrix to have a more effective contribution during the fracture. The stronger interphase subsequently results in 183% improvement in mode I and 75% improvement in mode II interlaminar fracture toughness of the composite.

1. Introduction

Delamination is still considered to be the most dominant and life-limiting failure mode in the laminated composites. While continuous fiber reinforced polymer (FRP) composites exhibit excellent in-plane properties, delamination growth degrades the material and eventually results in their premature failure. Being susceptible to delamination considerably restricts their in-service applications including primary aircraft and automotive structures. Improving the interlaminar adhesion and delamination resistance is specifically important in parts experiencing impact loading, under which cracks initiate and grow in the interlaminar region due to the contribution of mode I (opening), mode II and mode III (shearing) failure modes. In this regard, several strategies have been proposed to increase the interlaminar fracture toughness in FRP composites, including optimizing ply stacking sequence [1], interleaving the plies by a tougher polymer or micro- and nano-fillers [2–6] as well as through-thickness reinforcement (i.e., stitching [7], weaving

[8], z-pinning [9]). In addition, adding toughening modifiers, including rubber particles, silica particles, and carbon nanoparticles to the polymer (mainly epoxy) has been a prevalent approach to improve the interlaminar toughness and the impact damage resistance [10,11].

It has been shown that fibers have a significant contribution during the delamination process as the fracture toughness of the composite is commonly greater than the bulk epoxy owing to the provoked toughening mechanisms both ahead and behind the crack tip, such as fiber bridging and rupture as well as crack arrest and deflection [12]. The fiber—matrix interphase is the transition region which mechanically and chemically connects the bulk fiber and bulk matrix in the composite. The formation of this phase is influenced by physicochemical features of both fibers' surface, e.g. carbon fiber (CF), and the matrix. Weak interfacial adhesion between the CF surface and epoxy has been a major limiting factor in developing the CF composites with theoretical mechanical performance [13,14]. The weak adhesion is attributed to low surface energy, non-polar, chemically inert, and smooth surface of CFs

E-mail address: amir.asadi@tamu.edu (A. Asadi).

^{*} Corresponding author.

¹ These authors contributed equally to this work.

[15]. The fiber–matrix interphase directly determines the effectiveness and distribution of load transfer between the fiber and matrix. It has been shown that in the case of most failure modes, including delamination, the main crack propagation occurs across the fiber–matrix interface [16]. Improving the interfacial strength not only enhances the system integrity and increases the ultimate strength [13,15,17–22], but it also enhances the interlaminar fracture toughness [23–26] by taking advantage of the potential toughness lying in the polymer matrix, which is mostly left unused due to the early fiber–matrix debonding [27].

The quality of formed interphase is determined by multiple factors including the extent of chemical bonding, mechanical interlocking, and fiber wettability of the fiber by resin [28]. The rough morphology of the fiber surface is associated with a better mechanical locking of the fiber and polymer after curing. The degree of chemical bonding between the fiber and polymer is influenced by the number of available reaction sites on the CF to react with epoxy. Planting functional groups such as carboxyl, amino, epoxy and hydroxyl on CF surfaces have been a prevalent method for increasing the chemical bonding [29]. Adjusting the polarity difference between the CF and polymer is also an important factor as it determines the extent of resin-fiber wetting and contact, which controls the intensity of voids in the interface [28,30]. Chemical grafting [31], plasma treatment [32], chemical vapor deposition (CVD) [33], and electrophoretic deposition (EPD) [34] are the main developed techniques that have been explored to modify physical and chemical features of the CF surface. The main drawback associated with these techniques is the need for lab-scale cost and/or time inefficient treatments on the CF, which cause challenges in scaling up the method [35-37]. Using nanoparticles has been an effective technique to engineer physical and chemical mechanisms involved in the fiber-matrix interphase. For instance, carbon nanotubes (CNT), and graphene have shown to increase the available surface area, stiffen the interphase region, and facilitate a smoother transition of mechanical properties in the interphase region, which will soothe stress concentration effect in the interphase [38]. Long CNTs have been shown to establish strong mechanical interlocking with epoxy, which occurs through CNTs tails on the carbon fiber surfaces extending into the epoxy matrix and leads to micromechanical interlocking effect at the interphase that in turn enhances the fiber-matrix interactions. This facilitates the efficient load transfer from reinforcing fiber to matrix and modifies the failure nature of the material. The enhanced localized plastic deformation, crack deflection, bridging gaps and pores, particle debonding and pull-out have been observed as key energy dissipating phenomena through which CNTs increase the fracture toughness [39-41]. Modifying the polymer matrix with nanoparticles is another strategy that has been adopted to mitigate the delamination failure, however, low viscosity of the modified resin and the challenges in fabricating high volume fraction composites (>60 vol%) as well as problems in achieving a uniform dispersion due to the filtering effect, which segregate and deplete the nanoparticles, are concerns that limit this strategy for engineering applications [42]. Further, it has been widely agreed that increasing toughness of the matrix above a certain threshold cannot effectively be transformed into the interlaminar fracture toughness of the fiber composite [43,44]. A common proposed strategy to toughen the matrix by promoting plastic deformations is decreasing its yield strength [45], however, these methods typically lower the system stiffness and strength, which is not generally desirable. This makes engineering the fiber-matrix interphase a more effective strategy than modifying the polymer matrix. The increase in the interfacial strength is expected to not only enhance fiber-related toughening mechanisms but also provide a more effective toughness transfer from matrix into the interlaminar fracture toughness.

The high surface area and strong van der Waals forces cause CNTs to agglomerate into bundles. This can be reflected in several studies in which adding any amount of CNT decreases the fracture toughness [46]. Hence, proper dispersion and avoiding secondary agglomeration before integrating is crucial for taking advantage of CNTs excellent intrinsic

properties. In this regard, carbon nanoparticles are chemically functionalized, and/or hybridized by other functional nanoparticles to exert their superior mechanical properties to the most. Graphene oxide (GO) is a common form of modified graphene that offers abundant functional groups on the graphene surface [47]. Use of mixed sulfuric and nitric acids (H2SO4/HNO3) have also been a prevalent method for chemically functionalizing the carbon-based nanoparticles [48]. It should be noted that besides the lack of scalability, doing functionalization on CNT, which usually involves intensive processes, has been shown to damage CNT sidewalls, deteriorating their mechanical performance [49,50]. CNTs have been hybridized with different classes of materials to achieve synergistic enhancement of properties in the resultant hybrid nanocomposite [51–53]. A number of efforts have covalently grafted polymer chains onto the graphene and CNT to disperse them and make a hybrid nanostructure [54]. Shariatnia et al. [55] recently developed a technique for integrating pristine CNTs (pCNTs) on the CF surface with the aid of cellulose nanocrystals (CNCs) and showed that hybridizing 0.2 wt % CNC and 0.2 wt% CNT on the CF surface yield 33% enhancement in flexural properties, and 35% in interlaminar shear strength. It was reported that this improvement is unattainable by using the individual CNTs or CNCs due to the synergistic strengthening mechanisms which appear when CNTs and CNCs are used together. CNCs exhibit high aspect ratio, low density, low toxicity, and numerous accessible hydroxyl side groups (-OH) as hosts for different nanoparticles [56,57], which makes them good candidates to be used as chemically assistant

Numerous experimental and numerical studies have attempted to improve the fiber-matrix interfacial properties and study its influence on the fracture toughness of the carbon/epoxy composites [24,29,58-62]. In a recent study, CF was coated with CNTs that were pre-treated by grafting cationic polymers on them. Compressive and short beam shear strength as well as mode I interlaminar fracture toughness of the fabricated composites were investigated in this study [62]. Although several studies have dealt with this subject, most of them only address the influence of surface treatment on macroscopic properties of composites. A comparative experimental study on the role of CF surface topological and chemical properties on strength of the formed interphase, and its relation to the fracture toughness, and crack initiation and propagation response in the CFRPs is missing. Hence, the relationship between the interphase properties and fracture toughness is not well understood. The proposed combination of nanoparticles in this study, that offers different physicochemical properties, enables a deeper insight into the nature of the interphase formation. In addition, the potential of CNCs united with CNTs in improving the interlaminar fracture toughness has not been explored yet. This is an interesting synergy since CNCs act both as dispersing, coating agent and also a chemical agent during the subsequent interphase formation.

This paper aims to reveal how chemical and mechanical properties of the fiber-matrix interphase affect the interlaminar fracture toughness of carbon fiber reinforced polymer (CFRP) composites. We modify the fiber-matrix interphase by three combinations of nanomaterials and study its relation to the mode I and II interlaminar fracture toughness of CFRP composites. The CF surface is modified by incorporating functionalized CNTs (fCNTs), CNCs, and CNC-CNTs (pristine CNTs). To coat the fibers with pristine CNTs, we use the previously developed method in our group, i.e. delivering pristine CNTs using CNCs on the fiber surfaces through aqueous immersion [55]. Single fiber fragmentation (SFF) tests, double cantilever beam (DCB) and end-notched flexure (ENF) tests were used for measuring mode I and II interlaminar fracture toughness, respectively. Using the AFM nano-IR method, a comparative investigation on the topology and the chemical properties of the interphase with different coatings was performed to understand how interfacial features influence the interlaminar fracture response of CFRPs.

2. Experimental

2.1. Materials

The CNCs used in this work are NCV-100 CNCs (CelluForce, QC, Canada) with a diameter of 3–4.5 nm, length of 44–108 nm, and molecular formula of $[(C_6O_5H_{10}]_{22-28}SO_3Na]_{4-6}.$ Pristine multi-walled CNTs produced via catalytic CVD with 95% carbon purity and average outer and inner diameters of 5–15 nm and 3–5 nm and length of $\sim\!10~\mu m$ are purchased from US Nano (United States). Unidirectional (UD) Hexcel IM2 CFs (12 k tow size) are used as received. Epoxy INF-114 and INF-211 hardeners are supplied from Pro Set (USA). Functionalized CNTs (fCNTs, AQUACYL^TM AQ0302) are purchased from Nanocyl that are 3 wt % acid hydrolyzed CNTs dispersed in aqueous solution.

2.2. Coating procedure and composite manufacturing

A schematic of processing-fabricating steps for making CNC, fCNT, and CNC-CNT modified CFRP composites are shown in Fig. 1. 12 and 16 layers of CFs were used for making the laminates for DCB and ENF tests, which resulted in laminates of 3.1 mm and 4 mm thicknesses, respectively. Unidirectional composite laminates were manufactured with four different coated CFs: (i) uncoated (ii) fCNT coated, (iii) CNC coated, (iv) CNC-CNT coated. Using individual pristine CNTs was not feasible in this study as the CNTs agglomerate in the water without dispersants. Instead, nitric-sulfuric acid treated fCNTs were used, which is an established class of CNTs due to their compatibility with the polymers and stability in solvents. The coating process was performed by immersion coating method at which the CF fabrics were immersed in a bath of prepared suspension for 20 min followed by drying in an oven at 90 °C overnight. The coating suspension for all the cases is prepared by dispersing the nanoparticles in deionized water (DI-H2O) using probe sonication for 30 min with the cycle of 20 s pulse on and 10 s pulse off at 20 kHz and 75% intensity within an ice-bath. The concentration of all suspensions is 1 wt % and the ratio of CNC-CNT suspension is 10:1 (CNC's weight is 10 times that of CNTs'), according to our previous study [55]. The coating process parameters including solution concentration, CNC-CNT ratio as well as

sonication and immersion time is adopted according to the prior attempts [55,63]. During the sonication, small CNC nanoparticles tend to infiltrate and attach to the CNTs. Electrostatic attraction and polar- π interactions between the carbon rings of CNT and the CH groups in cellulose, and covalent bonding between the OH and sulfate groups of CNCs with the defected sites of CNTs are the main binding/bonding mechanisms of CNC-CNT [57]. Formation of hydrogen bonds between CNC and water molecules and the strong interaction between the CNT and CNCs prevents the CNC crystals from re-agglomeration after stopping the sonication and stabilizes the suspension for months. In fact, the attached CNCs to CNTs act like functional groups such as carboxyl and hydroxyl groups on functionalized CNTs. Moreover, the used sulfuric acid treated CNCs have shown to have negatively charged sulfate halfester groups that results in colloidal stability [64-66]. To manufacture the hybrid composites, vacuum-assisted resin transfer molding (VaRTM) process was used. Artificial pre-cracks were created using 20 µm thick Teflon film, which was placed in the midplane of the laminate prior to resin infusion. The CFRP laminates were cured at 60 °C for 8 h on a sealed hot plate. It is noted that fabricating hierarchical composites via autoclave method will have relatively higher mechanical properties compared to VaRTM due to better resin diffusion and fiber wetting [67], however, we hypothesize that it will not impact the observed trends in this research as the void volume fraction of fabricated specimens are around 2.5%, see supplementary information.

2.3. Mechanical testing procedure

The DCB and ENF tests were performed according to the ASTM D5528 [68] and ASTM D7905 [69] to measure mode I and II fracture toughness, respectively. DCB specimens with the geometry: width =25 mm, thickness =3.1 mm, total length =150 mm, and ENF specimens with the geometry: width =25 mm, thickness =4 mm, total length =140 mm are shown in Fig. 2. The pre-crack lengths in the DCB and ENF specimens are 60 mm, and 45 mm, respectively. For DCB samples, piano hinges were attached to the two sides of specimens in a way that the distance of initial crack tip to the loading point was 20 mm. As the crack opening distance increased, delamination propagated along the mid-

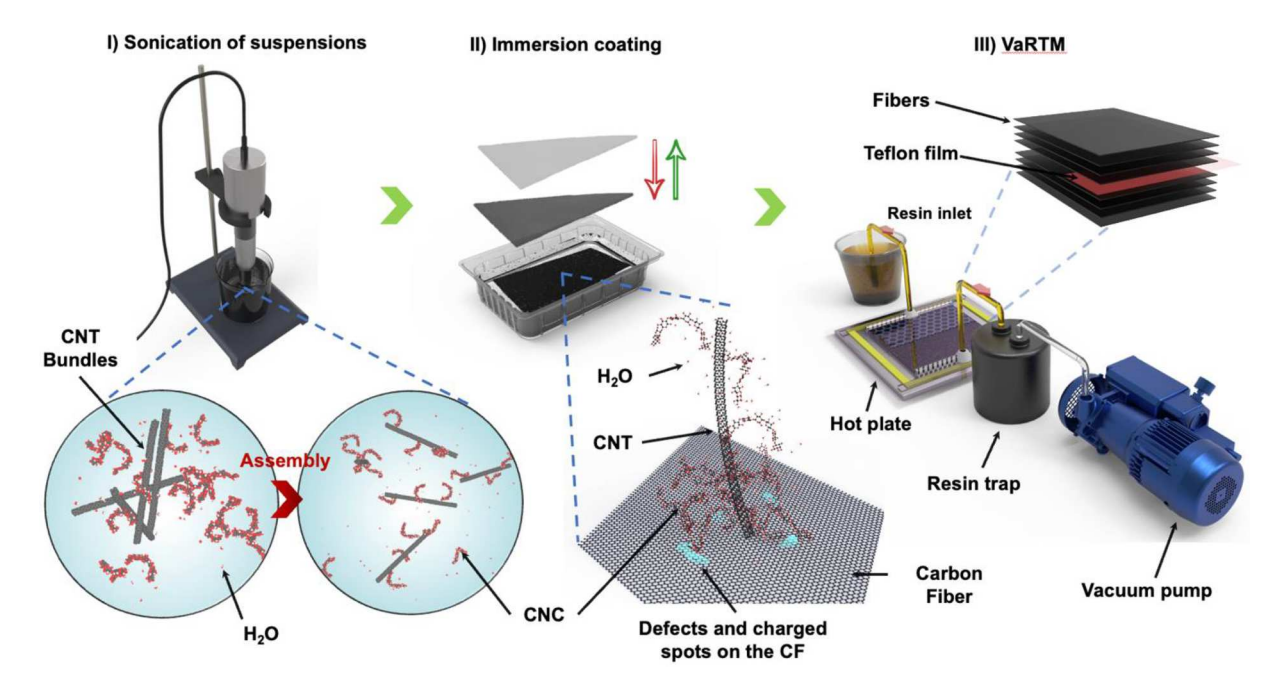


Fig. 1. Manufacturing steps for coating carbon fibers with CNC-CNT nanoparticle system, and fabrication of composite laminates: i) aqueous solution of nanoparticles are sonicated during which CNT-CNC assembly is built and stabilized in the water. ii) CNC-CNT nanostructures are attached to the carbon fiber surface by the defected sites and locally charged regions. iii) the coated fibers are stacked with a Teflon film, as artificial crack, and vacuum assisted resin transfer molding (VaRTM) method is used for making composite laminates. It is noted that the same technique was used for fabricating laminates for the fCNT and CNC specimens.

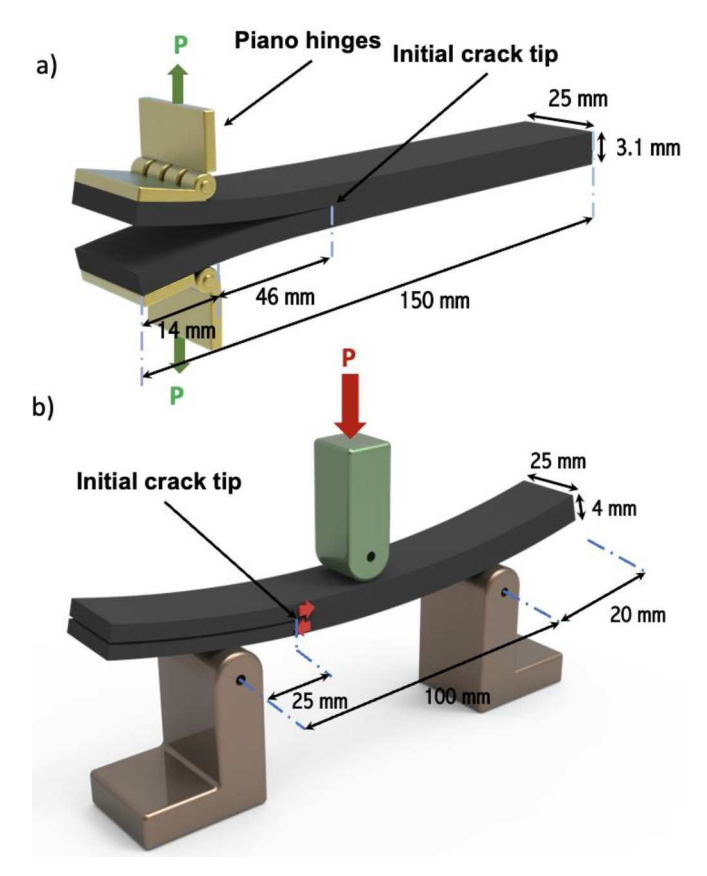


Fig. 2. a) geometrical dimensions of the fabricated DCB specimens including total length, and distance between the loading axis and the crack tip. b) the configuration of enf test including span length and crack tip position.

plane of the specimens. The applied load, crack opening displacement and crack length were measured in steps during DCB and ENF tests. Sides of the specimens for both DCB and ENF samples were painted by a white, solvent-based paint and marked to permit tracking of the crack-tip location. The tests were performed using a UNITED SMART 1 testing machine under displacement control condition with a crosshead speed of 10 mm/min. Seven samples were tested for each case and the delamination crack growth was recorded using a digital camera for post-processing.

2.4. Data reduction schemes

The mode I and II interlaminar fracture toughness, which are indicators of required energy for the unstable crack to grow, for each increment was calculated according to the modified beam theory (MBT). According to this method, mode I interlaminar fracture toughness, G_I , is calculated as:

$$G_I = \frac{3P\delta}{2b(a+|\Delta|)}\tag{1}$$

where P= applied load, $\delta=$ crack opening displacement in the load point, b= sample width, a= crack length, and Δ is a correction factor for the crack length and calculated according to ASTM D5528. The mode II initiation interlaminar fracture toughness, G_{II} , is calculated based on the direct beam theory (DBT) as:

$$G_{II} = \frac{9P\delta a^2}{2b(2L^3 + 3a^3)} = \frac{9P^2a^2C}{2b(2L^3 + 3a^3)}$$
 (2)

where P = maximum load level, L = span length, a = crack length, b = specimen width, and δ = maximum displacement. It is noted that an

initiation value for the onset of crack growth, and an interlaminar fracture energy value for the steady state crack propagation is obtained and reported separately.

2.5. Single fiber fragmentation (SFF) tests

Single fiber fragmentation (SFF) tests are conducted to evaluate interfacial strength of modified CFRPs using a Kammrath Weiss 10 kN micro tensile stage under an optical microscope (DXS 500 by Olympus). The SFF specimens are prepared by embedding a single filament extracted from a coated CF tow into the dog-bone-shaped silicone mold filled with epoxy resin, and cured under the same conditions of CFRP composites. The dog-bone shape samples are 50×10 mm with a gauge length of 25 mm. The interfacial shear stress (IFSS) values are calculated by Kelly and Tyson [70] model in Eq. (2):

$$\tau = \frac{d_f \sigma_f}{2l_c} = \frac{3d_f \sigma_f}{8\bar{l}} \tag{3}$$

where τ is interfacial shear strength (IFSS), d_f is the fiber diameter, l_c is the critical length, and σ_f is the fiber tensile strength at critical length. The critical length, l_c , is calculated using $l_c = \frac{4}{3}\bar{l}$, where \bar{l} is the average fiber length. An average of 6 samples is reported. Weibull distribution used for the carbon fiber strength data (according to ASTM D3822) were applied to obtain Weibull shape parameter and strength as 4.91 and 4038 MPa, respectively. Note that the individual fibers are pulled out from the coated CF tow.

2.6. Atomic force microscopy (AFM)-infrared (IR) spectroscopy and scanning electron microscopy (SEM)

The AFM Nano-IR (Bruker Anasys nano-IR2) is conducted to understand the topological and chemical features at the CF-epoxy interphase. AFM-Nano-IR simultaneously probes both topology (AFM) and evolution of the chemical composition of the interphase (IR) of CFRP composites coated by different nanoparticle systems. The specimens are prepared by inserting and taping a CF tow on top of a silicone holder $2\times5\times1$ cm poured with epoxy. To obtain a smooth surface, CFRP is grinded using 400–7000 grit sandpapers and polished with aluminum particles of 6 μm size. The AFM micrographs are collected at AFM tapping mode and taken from the top view and the measurements are conducted for at least 3 samples for each composite. The IR measurements are performed in the range of 1800–800 cm $^{-1}$ with 20 nm spatial resolution. The tips have a nominal radius of 30 nm, according to the manufacturer (Bruker Anasys nano-IR2).

Fracture surface investigation was performed using scanning electron micrscope (SEM) (Tescan FERA-3 Model GMH Focused Ion Beam Microscope) with an acceleration of 5 kV. Before SEM, the surfaces were sputter-coated with 5 nm gold to increase the conductivity of the surface.

3. Results and discussion

3.1. Fiber-matrix interphase features

Characterizing chemical and physical properties of the formed interphase between the epoxy and modified CFs provides important information for interpreting the mechanical response of the interphase. The interfacial region of CNC, fCNT, and CNC-CNT coated CFRPs are evaluated using AFM-NanoIR, as presented in Fig. 3. The technique is composed of AFM and IR with a spatial resolution of 20 nm that allows revealing the chemical composition of the interphase at a nanoscale resolution for adhesion studies. IR data was captured from the epoxy (red), interphase (green) and CF surface (blue) as depicted in AFM micrographs in Fig. 3a. In the uncoated sample in Fig. 3a, there is no significant interphase captured as the plot jumps by 600 nm in Fig. 3i. On

Composites Part A 166 (2023) 107390

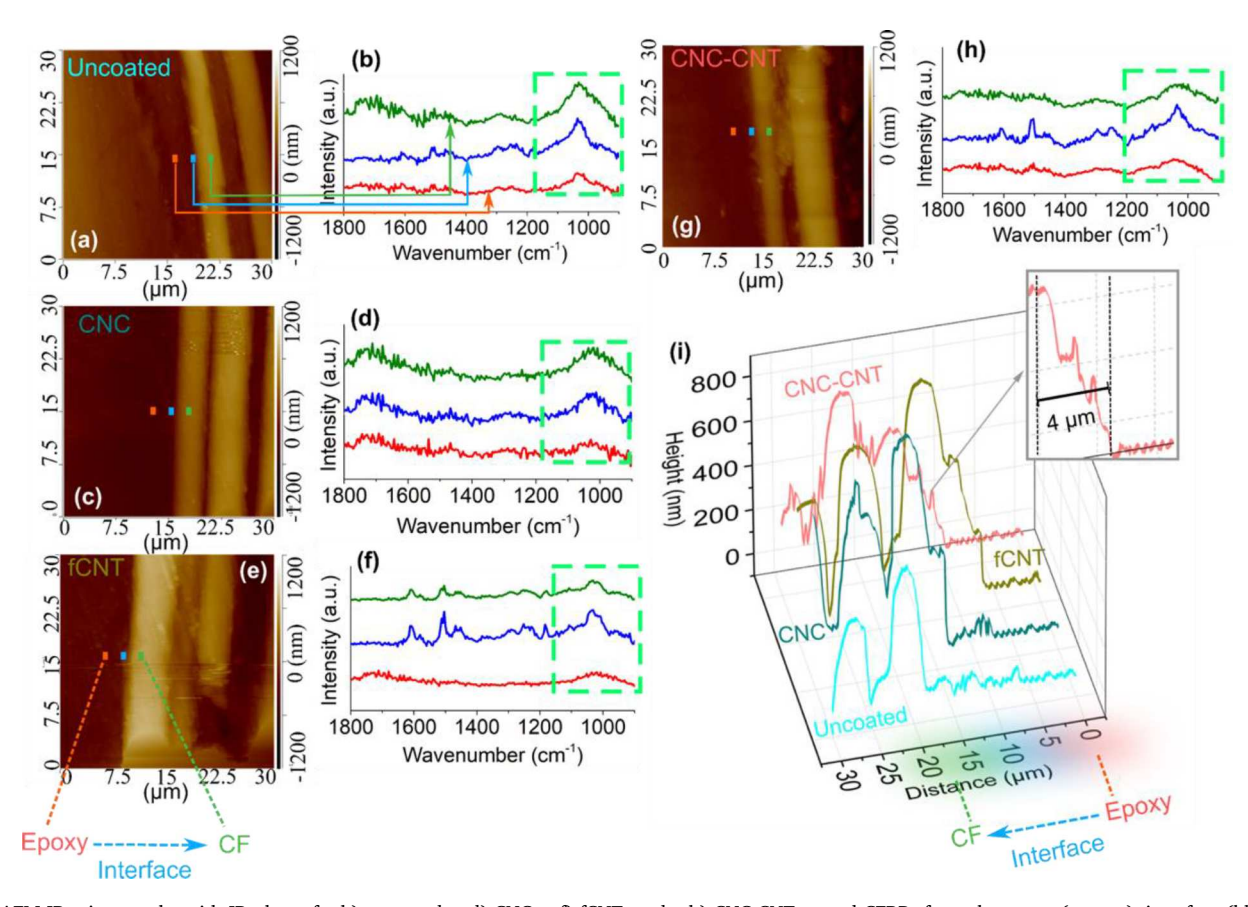


Fig. 3. AFM-IR micrographs with IR plots of a-b) uncoated, c-d) CNC, e-f) fCNT, and g-h) CNC-CNT coated CFRPs from the epoxy (orange), interface (blue), and carbon fiber (green). The green dashed box in IR plots point out the change in the polar group in 1040 cm⁻¹ from epoxy (red) to interface (blue) and carbon fiber (green). (i) AFM height-distance plot of uncoated, CNC, fCNT and CNC-CNT coated CFRPs. The magnified region in (i) presents the gradual carbon fiber-epoxy interface change in CNC-CNT coated CFRP. (For interpretation of the references to colour in this figure legend, the reader is referred to the web version of this article.)

the other hand, AFM height versus distance plot in Fig. 3i shows a step-by-step rise from epoxy to carbon fiber, where about 2 μm gradual interfacial transition was captured in CNC and fCNT coated specimen in Fig. 3c and e, respectively. The wider interfacial transition zone becomes more pronounced in CNC-CNT coated specimen, where there is a 4 μm gradual interfacial region in Fig. 3i. The magnified region of Fig. 3i displays the gradual height change of the CF-epoxy interphase due to CNC-CNT modification. This indicates that the synergistic effect of hybrid CNC-CNT provides a larger interfacial region compared to those of CNC and fCNT allowing smoother and more effective stress transfer from the matrix to fiber.

The IR spectra between 1800 and 900 cm⁻¹ are also presented in Fig. 3. The oxygen-containing peak, 1040 cm⁻¹ (C–O), boxed in Fig. 3b, 3d, 3f, and 3h reveal the interfacial interactions between epoxy and the coated CF. The intensity of the C-O group of the uncoated specimen (Fig. 3b) shows no considerable increases when approaching the CF from epoxy (from red towards the blue and green in Fig. 3a). This indicates a limited interaction between CF and epoxy, which is in accordance with the height-displacement plot that shows no interfacial region in Fig. 3i. In contrast, CNC coating (Fig. 3d) in CFRPs increases the relative C-O peak, especially at the interphase region (blue) and the CF surface (green) shown in Fig. 3d. This implies that CNC interacts with both CF surfaces as well as with epoxy due to the existence of hydroxyl and half-ester sulfate functional groups. fCNT coated specimen exhibits a similar trend in Fig. 3f. In this case, fCNT was decorated with -COOH as a result of the chemical functionalization process to improve the surface hydrophilicity of CNTs, and to create bonding with epoxy. Hence, the increase in the C-O peak is attributed to the enhanced

interaction with CF and epoxy due to the free -COOH bonds on the fCNT surface. In the CNC–CNT specimen (Fig. 3h), the dominant C–O peak at the interphase suggests the formation of more chemical bonds at the interphase possibly due to the bonding between CNC and CNT as well as the synergistic effect of CNC and CNT that provides both chemical (from CNC) and mechanical (from CNT) reinforcement leading to improved interfacial interactions of epoxy and CF. The increase in the interaction sites due to the company of CNTs improves the adhesion across CF-CNT-epoxy. IR spectra results also correlate with the obtained 4 μ m interfacial region in AFM images where the gradual transition is observed at the interphase in Fig. 3i. Overall, the CNC–CNT specimen exhibits increased polar bonding (e.g., C–O) at the interphase region along with a wider and gradual interphase formation, indicating the formation of strong interfacial adhesion between the CF and epoxy.

3.2. Interfacial shear strength (IFSS) of coated CFRPs

Interfacial properties of materials dictate the comprehensive mechanical properties, fracture mechanisms, and delamination performance of CFRPs. According to the shear lag model, homogeneously dispersed nanomaterials at the interphase allow a gradual stress transfer from the matrix to reinforcing fibers. To understand the effect of CNC, fCNT, and CNC-CNT addition on IFSS, the SFF test is conducted as described in Section 2. The results are presented in Fig. 4, where IFSS and l_c refer to interfacial shear strength and the critical fiber length that carries the load, respectively. As expected, l_c values steadily reduce from 630 μ m (uncoated CFRP) to 392 μ m (CNC-CNT coated CFRP) when the interfacial strength of CFRPs is enhanced with the addition of

Composites Part A 166 (2023) 107390

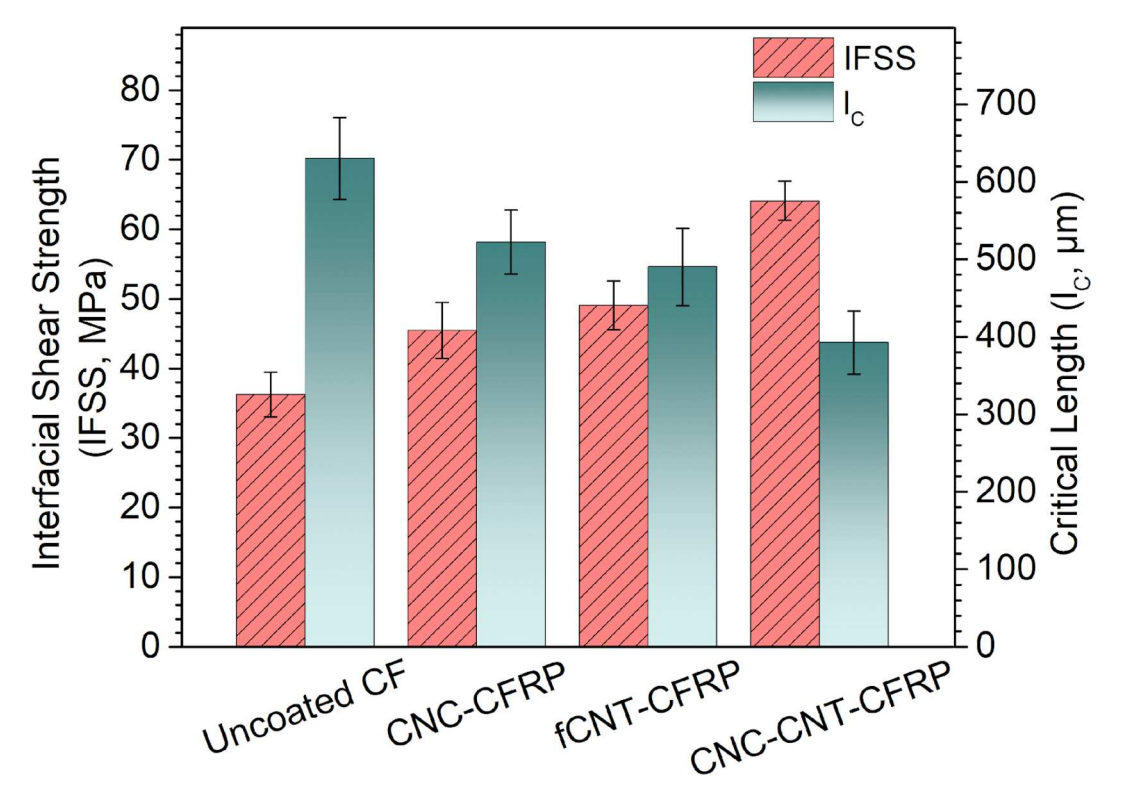


Fig. 4. Interfacial shear strength, IFSS (red) and the critical fiber length, lc (green) of fibers modified with CNC, fCNT and CNC-CNT. (For interpretation of the references to colour in this figure legend, the reader is referred to the web version of this article.)

nanomaterials. IFSS value is 36 MPa for uncoated CFRP, and it gradually increases with the addition of CNC (45 MPa), fCNT (49 MPa), and CNC-CNT (64 MPa). The enhanced interfacial strength for CNC, fCNT, and CNC-CNT modified CFRPs compared to uncoated CFRP's correlates with the increase of interfacial zone from ~ 0 to 2 and 4 μm , respectively, probed in AFM Nano IR in Fig. 3i. This is attributed to the fact that once the epoxy resin is infused, we expect that a number of CNTs' (with CNCs attached) tails flow through the epoxy matrix while the head is bonded to the carbon fiber surface. Since our epoxy system (INF-114) is diglycidyl ether bisphenol A based, the functional groups of CNCs (e.g., hydroxyl groups and half-ester sulfate groups) react with epoxides and form covalent bonding that generates strong interactions with the epoxy matrix [71]. As a result, a number of CNTs (with CNCs attached) act as nanobridges between carbon fiber and epoxy and several of them disperse through the matrix. This allows to achieve both interfacial enhancement and toughening of the composite system. A significant IFSS enhancement in CNC-CNT modified CFRPs is associated with the synergetic effect of CNC and CNT and that is both chemical (from abundant side groups of CNC and C-O bonds, see Fig. 3h) and mechanical (presence of stiff CNTs) modification at the interphase as well as extended interphase (4 µm, Fig. 3i). Hence, presence of CNC enhances the material properties by two parallel mechanisms: (a) increasing the interfacial adhesion between the fiber and matrix, and (b) infusing the CNC-CNT into the epoxy. It is shown that the CNC-CNT coating on CF is able to provoke enhancements in the interfacial strength comparable to more intense modifications including plasma treatment [72], and considerably higher values compared to commercial sizing agents [73].

3.3. Mode I and II interlaminar fracture toughness — Delamination resistance

The DCB and ENF test results were analyzed to study the crack initiation and propagation of CFRPs with different coated fibers. Fig. 5 shows the mean values of mode I and II interlaminar fracture toughness (energy required for delamination) at crack initiation and propagation

and the corresponding load—displacement. Major forms of energy dissipation that occur during the delamination of fiber composites are matrix deformation, fiber bridging, interfacial debonding, fiber pull-out, and fiber breakage (see Fig. 6). The delamination resistance in both mode I and mode II for all the coated fiber composites is notably higher compared to uncoated CFRPs. The company of CNC and CNT results in an improvement greater than individual CNC or fCNT in the increase of energy onset for both interlaminar crack initiation and propagation in mode I and mode II (see Fig. 5a and 5d). In addition, Fig. 5c and 5e show that the initial slope of load—displacement curves in both mode I and II increase as the interfacial strength is improved (see Fig. 4). Fig. 6 depicts the toughening effects and mechanisms during mode I and II delamination of CFRP composites, and schematically represents the common patterns during the crack propagation.

As shown in Fig. 5c and 5e, the load required to initiate crack under mode I and II delamination is considerably altered with the change of the interphase. The increase in the maximum experienced load level under mode I delamination are 35%, 24%, 83%, for CNC, fCNT, and CNC-CNT modified CFRP composites, respectively. A similar trend is observed for mode II, where the percentage increases are 21%, 25%, and 45% for CNC, fCNT, and CNC-CNT, respectively (Fig. 5e). The required load for mode I and II crack initiation are governed by the extent of micro-cracking in the resin around the insert tip. Hence, the observed improvement can be attributed to the change in the pattern of microcrack growth at crack tip and the increased size of fracture process zone in different specimens, which also decreases the stress intensity at the crack tip, and provides a more efficient load redistribution far from the crack front. This is also reflected in the improved mode I and II crack initiation fracture toughness (Fig. 5a and 5d). The observed increase in the mode I fracture toughness at crack initiation ($G_{IC, initiation}$) are 71%, 50%, and 183% for CNC, fCNT, and CNC-CNT, respectively, compared to uncoated ones. The corresponding increases for mode II fracture toughness at crack initiation (G_{IIC, initiation}) are 18%, 29%, and 75%, respectively, compared to that of uncoated composites. The slightly higher mode I fracture toughness in the CNC compared to fCNT indicates

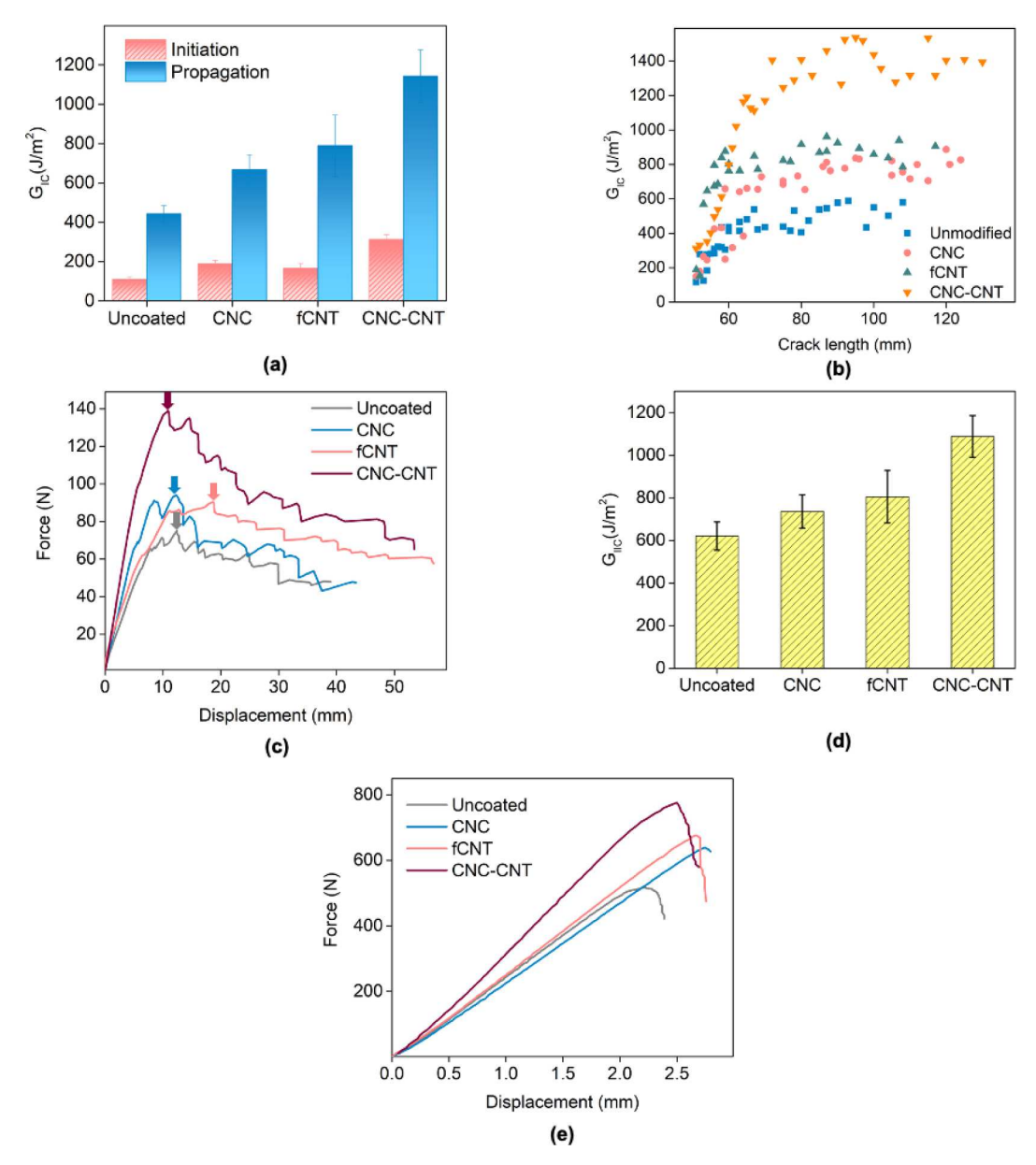


Fig. 5. (A) mean values of mode I interlaminar fracture toughness, G_{IC} , for crack initiation and propagation, b) R-curves showing resistance to fracture under mode I delamination in terms of crack extension, c) force—displacement graphs during mode I delamination, arrows show the corresponding maximum force for each case, d) mean values of mode II interlaminar fracture energy, G_{IIC} , for crack initiation, e) force—displacement plots of three point bending test for mode II delamination. The error bars depict the standard deviation.

that, similar to IFSS, improved fiber—matrix adhesion by CNCs is able to offer a relatively higher contribution in increasing the mode I crack initiation tolerance. This trend is reversed for mode II, where fCNT shows a higher crack tolerance. This is attributable to the relatively higher increase in the initial mode II delamination stiffness (Fig. 5e), caused by the restricting effect of stiff fCNTs in the interphase. The significant improvement of all delamination resistance properties for the CNC-CNT is due to the enhanced fiber—matrix chemical interaction by CNC as well as contribution of CNTs and CNCs in mechanical interlocking and thus building a stronger bonding across CF-CNC-CNT-epoxy. The locally toughened regions in the interphase are expected to arrest or deflect the initial microcracks (Fig. 6), which increases the tolerance of the main crack to initiate.

The increase in the mean values of mode I interlaminar fracture toughness during propagation ($G_{IC, propagation}$) were 50%, 78%, and 157%, for CNC, fCNT, and CNC-CNT, respectively (Fig. 5a). In addition, Fig. 5b shows the obtained G_{IC} values with respect to crack extension

under mode I delamination. It is evident that G_{IC} value of all cases increase gradually and tend to stabilize once the crack length reaches 65 mm. This steady fracture toughness is mainly due to the stabilization in the number of bridging fibers per unit crack area. It is noted that ENF test provides the mode II fracture toughness only for the crack initiation and therefore, crack propagation in mode II is not reported. The common 'stick-slip' response was observed for all the mode I specimens during the crack propagation (Fig. 5c); this response is due to presence of locally tough regions during the delamination that retards the crack growth until the elastic energy builds up again and initiates the next slip. It is evident that the steady state crack propagation values of mode I interlaminar fracture energy are higher compared to the corresponding initiation values. This considerable difference is mainly due to the effective contribution of crack resisting phenomena associated with fibers, especially fiber bridging, during the propagation (Fig. 6). Due to the extensive fiber bridging in mode I fracture of CFRPs, the load typically reaches a plateau for all the specimens (Fig. 5c). The increase in the

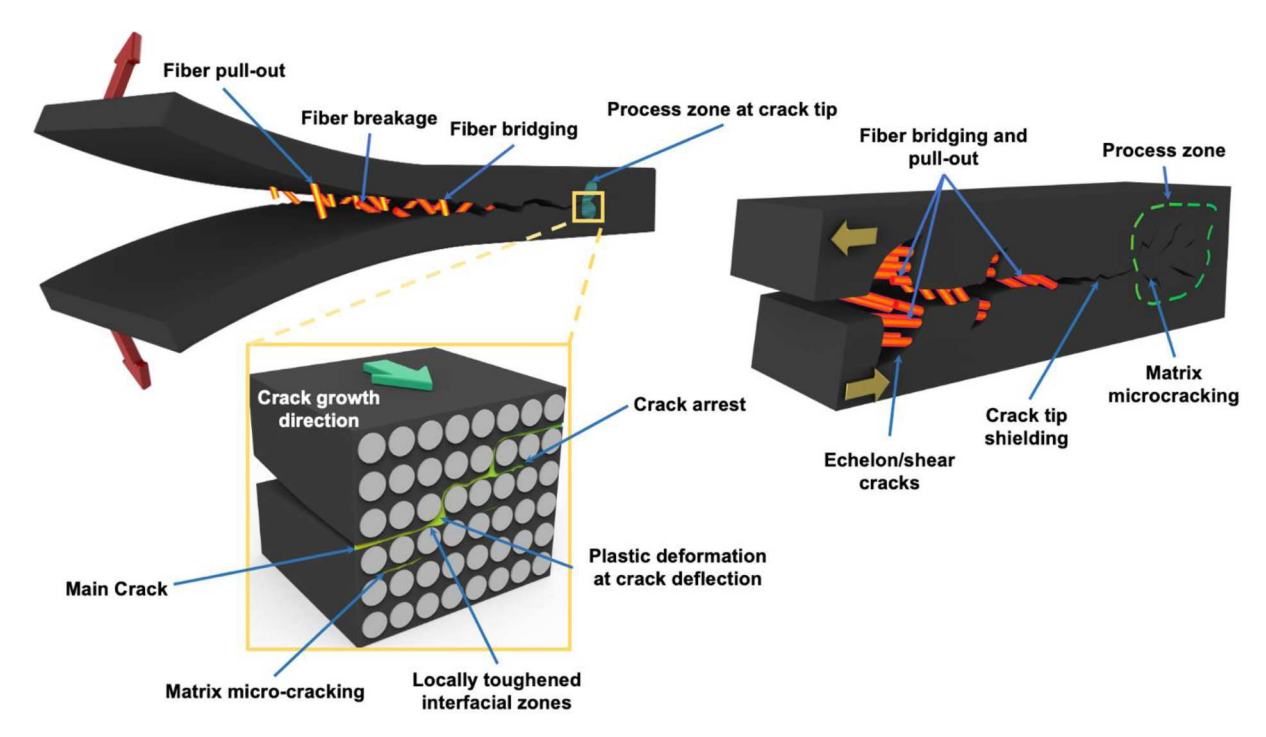


Fig. 6. Involved physical mechanisms and toughening effects during mode I (left) and II (right) delamination of fiber composites, and a schematic of crack path deflection patterns.

interfacial strength is expected to not only enhance fiber-related toughening mechanisms, due to the enhancement in crack deflection to the neighboring layers, but also provides a more effective toughness transfer from the polymer matrix. The improved fiber matrix strength provides the chance for the matrix to experience higher levels of stress during the crack propagation, which gives rise to energy-dissipating

events in the matrix, including enhanced plastic deformations.

The mean value of interlaminar fracture energy in mode I during steady state crack propagation increased from 443 J/m^2 for the CFRPs with uncoated fibers, to 1142 J/m^2 for the CNC-CNT CFRPs (see Fig. 5a), which can be correlated to physicochemical modification and enhanced IFSS (see Figs. 4 and 7). The modification of the interphase by CNC alters

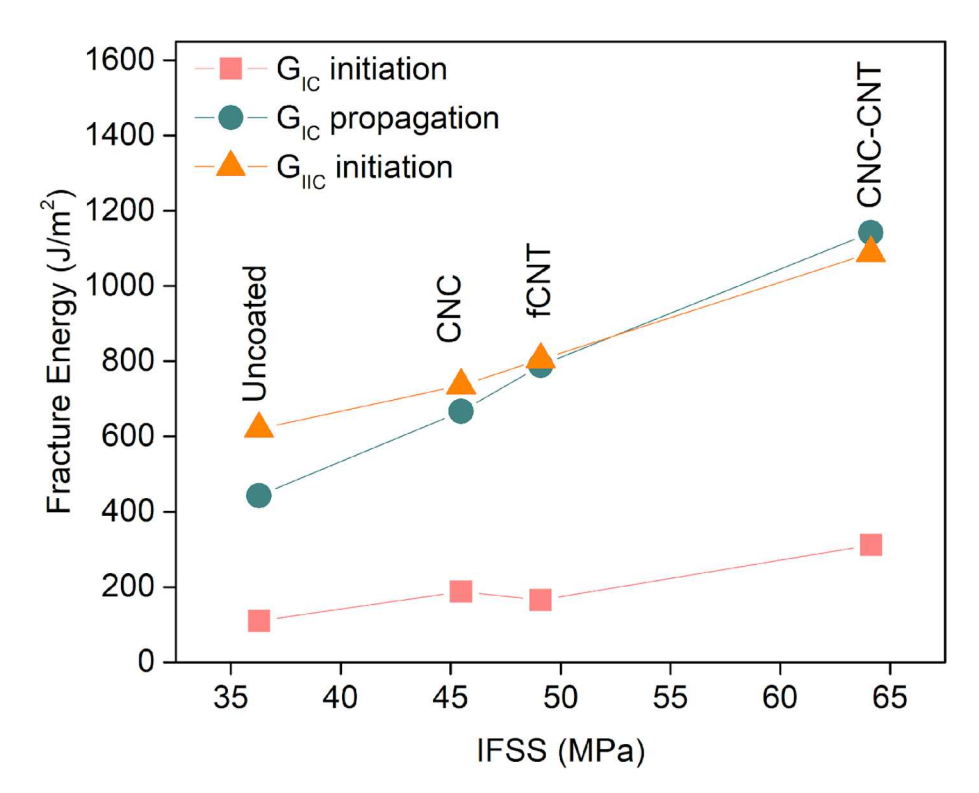


Fig. 7. The relation between interfacial shear strength, IFSS, mode I initiation fracture toughness, G_{IC} , initiation (pink), mode I propagation fracture toughness, G_{IC} , propagation (green), and mode II interlaminar fracture toughness, G_{IIC} (orange). (For interpretation of the references to colour in this figure legend, the reader is referred to the web version of this article.)

the crack propagation tolerance almost similar to the fCNT case. Further, it is observed that the CNC-CNT synergy in the fiber—matrix interphase is capable of enhancing the fracture toughness almost equivalent to interleaving thermoplastic veils into the carbon/epoxy composites [74,75], and higher compared to employing individual CNTs in the interlayer region [76]. Despite the interfacial strength and crack initiation tolerance, where fCNT showed slightly lower improvement compared to the CNC, the CFRPs with fCNT show higher energy dissipating capability during the mode I crack propagation. This is attributable to the better contribution of long, stiff fCNTs ($\times 10$ longer than CNC's) in provoking toughening mechanisms in the interphase including nano-bridging effect and crack deflection (Fig. 6). It is noted

that fCNT and CNC-coated fibers are both expected to promote shear yielding in the epoxy at the vicinity of the crack tip. The inadequate fiber–matrix bonding in the uncoated carbon fibers, however, is not able to provoke crack-resisting phenomena, which is characterized by smooth interlaminar fracture surface. The synergy of CNC and CNT shows to improve crack propagation tolerance more than individual CNC and fCNT. This is due to the presence of toughening effects arising from both CNC and CNT, i.e. the improved fiber–matrix adhesion by CNCs, and toughening effects associated with CNTs. This combination, as will be shown in section 3.3, results in a more pronounced deviations in the crack path during the growth, which will increase the effective fracture surface during the delamination, and with the expense of extra

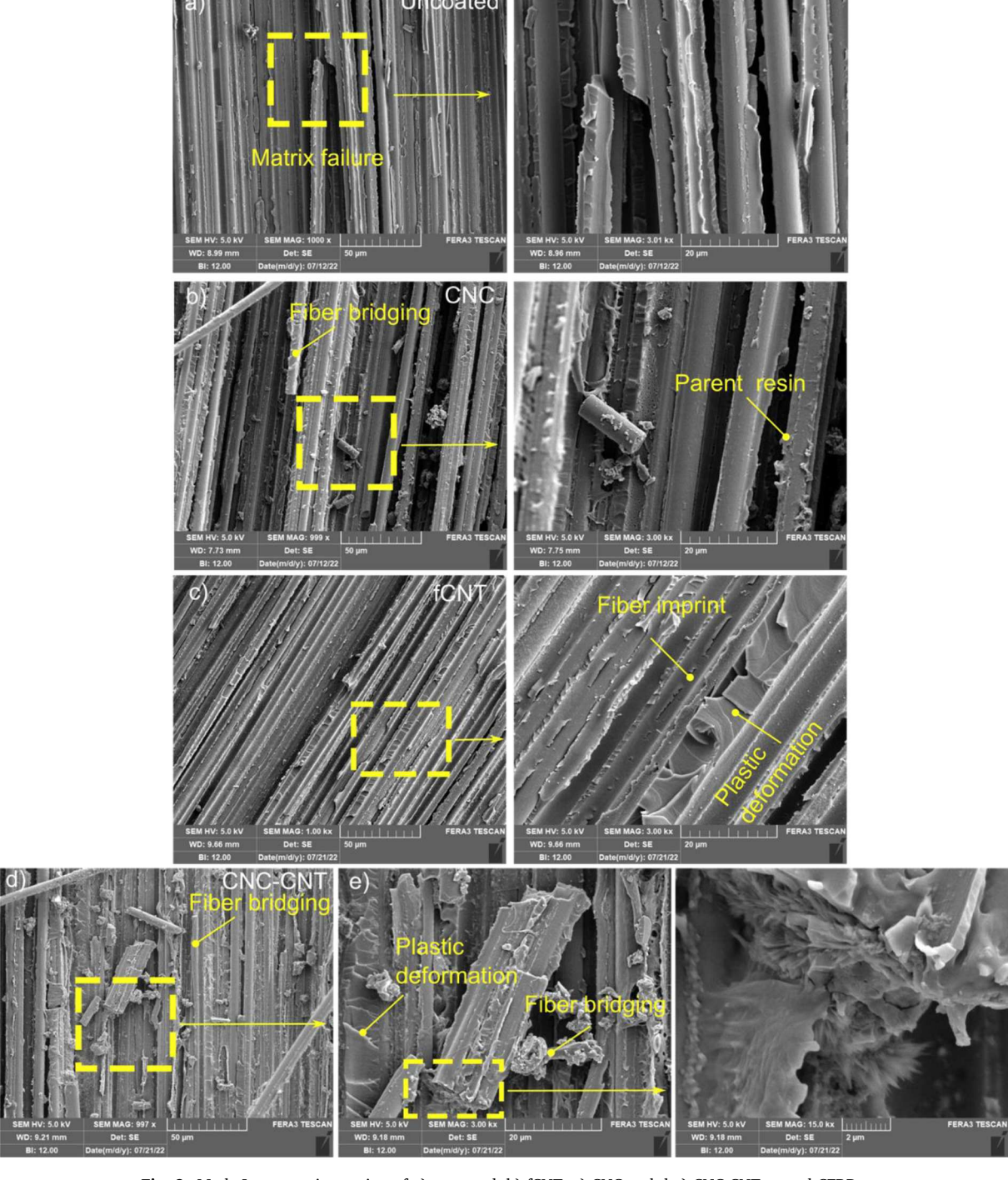


Fig. 8. Mode I propagation region of a) uncoated, b) fCNT, c) CNC and d-e) CNC-CNT coated CFRPs.

H. Fallahi et al. Composites Part A 166 (2023) 107390

fracture energy. Enlarging the size of the process zone at the crack tip accompanied by promoted crack arresting regions, will in fact increase the main crack's chance to deviate and pass through neighboring layers (see Fig. 6). These changes in the plane of the main crack front will also increase the number of involved fibers during the subsequent mode I crack opening, which results in a great energy dissipation.

The improved interfacial strength shows to considerably increase the crack initiation and propagation tolerance. Fig. 7 shows the correlation between the interfacial shear strength, IFSS, mode I crack initiation and propagation fracture toughness, $G_{IC, initiation}$ and $G_{IC, propagation}$, and mode II interlaminar fracture toughness $G_{IIC, initiation}$. It is seen that the improvement in the fiber–matrix interaction increases the interlaminar fracture energy by almost a linear trend. This is a result of enhanced toughening contributions of both the fiber and the matrix during delamination, which changes the interlaminar fracture characteristics. This also indicates the significant space that exists in the CFRPs for improving the fracture toughness by enhancing the chemical and mechanical interactions between the fiber and matrix.

3.4. Fracture surface morphology

The fracture surface of the propagation region in post-mortem DCB and ENF specimens was evaluated by SEM. Fig. 8 a-f presents the fracture surfaces of uncoated, CNC, fCNT and CNC-CNT coated CFRPs. Smooth fracture surface of the uncoated samples indicates that the crack initiation and propagation mainly occur in the midplane with minimum interruption as presented in Fig. 8a. Compared to uncoated specimens, CNC fracture surfaces in Fig. 8b present fiber bridging and crack deflection to the adjacent layers. In the high magnification SEM image of Fig. 8b, the resin residue on the fiber suggests the improved interfacial interaction of CNC-enabled CF and epoxy. Similarly, the fCNT fracture surface exhibits significant fiber imprints and resin plastic deformations, showing the toughening by long and entangled fCNTs (Fig. 8c). CNC-CNT coated CFRP specimens show a rougher fracture surface compared to that of CNC and fCNT coated CFRP composites (Fig. 8 d-e). Relatively, more notable fiber bridging and breakage as well as plastically deformed regions are evident. Crack path deflection due to the

improved fiber-matrix adhesion can promote CNT bridging effect and increase the number of broken CNTs during the delamination. Transverse cracking due to crack deflection will also considerably increase the fracture surface area. In the case of CNC-CNT coated CFRP specimen, a fibrillated feature appeared (see Fig. 8e), indicating accumulated shear cusps due to extensive plastic deformations. This feature can be attributed to the bridging of entangled CNTs during the delamination, suggesting that the interaction of CF and CNTs makes the CNC-CNT-CFRP composite tougher compared to that of fCNT-CFRP. The extent and presence of different modes in failure results in consumption of additional energy and retard delamination to higher stress level (see Fig. 5b). The fracture surface of the initiation region of post-mortem samples tested in mode I exhibits a similar trend (see Fig. 9). Uncoated (Fig. 9a) specimen shows minimal crack deflection compared to those of CNC (Fig. 9b), fCNT (Fig. 9c) and CNC-CNT (Fig. 9d). For the case of CNC-CNT, the unique fibrillated microstructure consisting of packed shear cusps is observed (see Fig. 9d and 9e). In addition to bridging effect of CNTs and better interfacial adhesion due to the presence of abundant -OH groups of CNCs, we hypothesize that the CNC-CNT at the interphase creates a resistance to crack initiation under mode I, which is manifested in the form of multiple and consecutive shear cusps.

Similar features are observed on the mode II fracture surfaces, as shown in Fig. 10. The fracture surface in the uncoated case shows crack deflection and more pronounced plastic deformation e.g., echelon shear cracks, and fiber imprints compared to mode I (Fig. 10 a-b); however, it is still relatively smooth compared to that of CNC (Fig. 10 e-f) and fCNT (Fig. 10 c-d) coated CFRPs. fCNT coated specimen shows more surface roughness and echelon features than that of CNC, probably due to effects provoked by long fCNTs. The more noticeable shear cusps in fCNT and CNC-CNT coated CFRPs (Fig. 10 f-h) compared to CNC-coated indicates the role of the CNTs and their entanglement contribution under shear deformation. It should be noted that roughness of fracture surface is an important factor in the mode II crack propagation, where a considerable portion of the shear load is carried by the friction and interlocking of asperities on the fracture surface behind the crack tip [77]. A schematic illustration of this effect can be seen in Fig. 6.

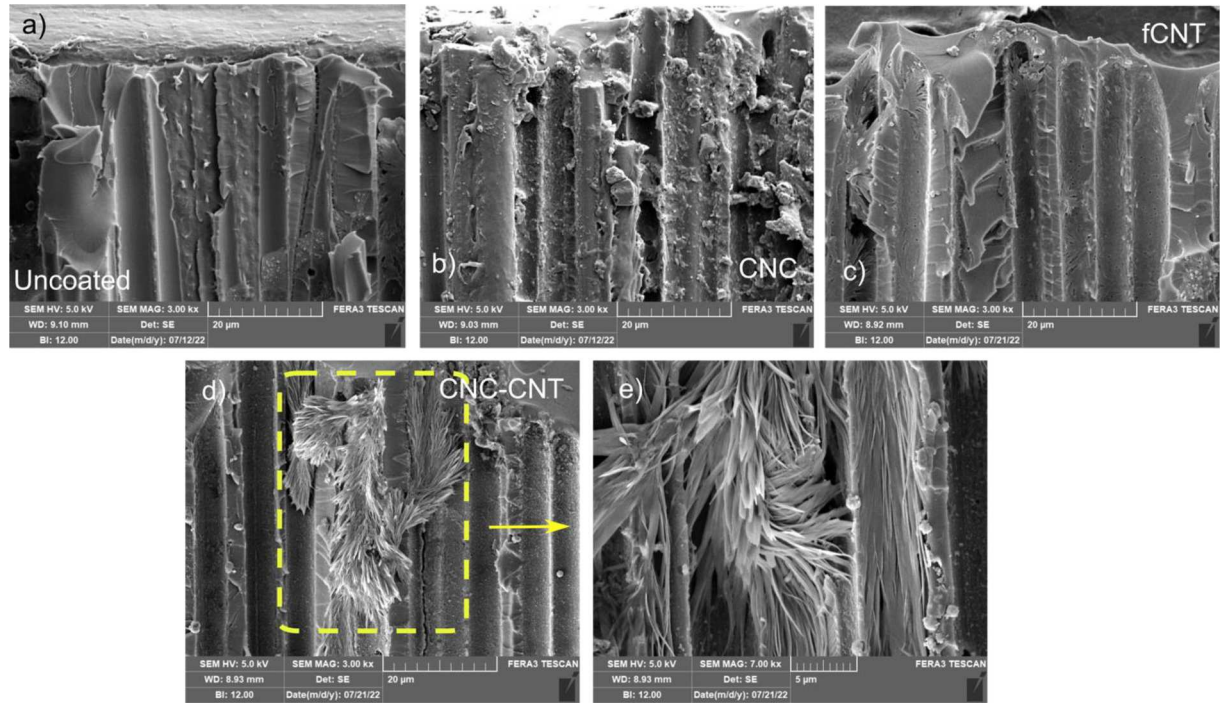


Fig. 9. Mode I initiation region of a) neat, b) fCNT, c) CNC and d,e) CNC-CNT coated CFRPs.

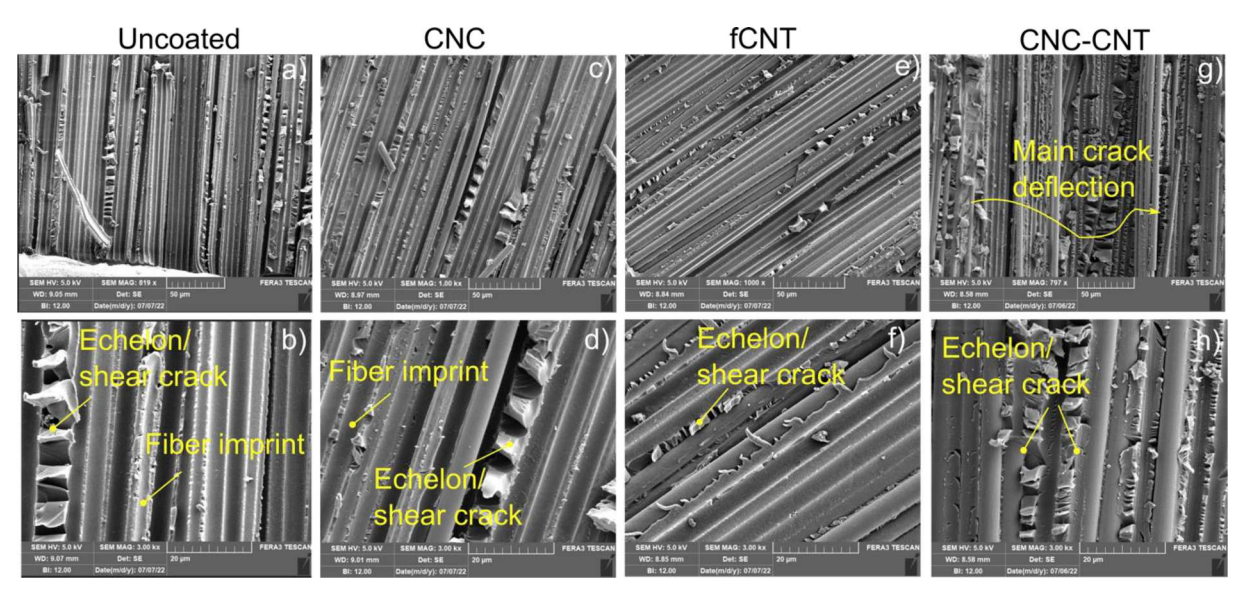


Fig. 10. Mode II crack propagation region of a,b) neat, c-d) fCNT, e-f) CNC and d-e) CNC-CNT coated CFRPs.

4. Conclusion

This work presented an experimental study on the relation of carbonepoxy interphase physicochemical features and the interlaminar fracture toughness. Modifying the carbon fiber surface showed to significantly change the delamination response of fabricated laminates. It was shown that improved interfacial interaction, mainly chemical bonding and mechanical interlocking, between fiber and matrix increases the interfacial shear strength and promotes active toughening mechanisms associated with both fiber and matrix, which increases the interlaminar fracture toughness. Results indicate that chemical engineering of the CF surface by CNC is able to improve the interfacial strength and interlaminar crack resistance almost equivalent to the fCNTs. The improvement in chemical bonding of carbon fiber and epoxy aroused considerable crack deflection during the delamination, triggering additional energy dissipating phenomena. Investigations on the width of the interphase zone revealed that CNC-CNT coating effectively widens the interphase zone from ~ 0 in uncoated CFPS to 4 μm in CNC-CNT-CFRP, which provides a more efficient load transfer between the fiber and matrix. In fact, CNC not only increases the interfacial adhesion between the fiber and matrix, but also helps the CNC-CNT to infuse into the polymer matrix enhancing the polymer matrix properties. Accordingly, crack initiation resistance was considerably improved due to the changes in the micro-cracking response in the vicinity of the crack tip. The capabilities of CNC-CNT synergy, which combines chemical features of CNC with mechanical features of CNT, showed the highest improvement in the IFSS by 76%, in the G_{IC,initiation} by 183%, G_{IC,propagation} by 157% and G_{IIC,initiation} by 45%, indicating the great potential of using hybrid nanostructures in engineering the carbon-epoxy composites. Our results show that using hybrid nanomaterials with different geometries and material properties allows engineering the physicochemical properties of the interphase effectively and synergistically enhance the interfacial and interlaminar strength in fiber reinforced polymer composites.

CRediT authorship contribution statement

Hamed Fallahi: Conceptualization, Methodology, Formal analysis, Investigation, Writing – original draft, Visualization. Ozge Kaynan: Conceptualization, Methodology, Formal analysis, Resources, Writing – original draft. Amir Asadi: Writing – review & editing, Supervision, Project administration.

Declaration of Competing Interest

The authors declare that they have no known competing financial interests or personal relationships that could have appeared to influence the work reported in this paper.

Data availability

No data was used for the research described in the article.

Acknowledgments

This material is based upon work supported by the National Science Foundation under Grant 1930277. The authors acknowledge the characterization part of this work was performed in Texas A&M University Materials Characterization Core Facility (RRID:SCR_022202). We also thank Nathan Santangelo for his help in fabricating composite laminates.

References

- [1] Caminero MA, García-Moreno I, Rodríguez GP. Experimental study of the influence of thickness and ply-stacking sequence on the compression after impact strength of carbon fibre reinforced epoxy laminates. Polym Test 2018;66:360–70. https://doi. org/10.1016/j.polymertesting.2018.02.009.
- [2] Daelemans L, Kizildag N, Van Paepegem W, D'hooge DR, De Clerck K. Interdiffusing core-shell nanofiber interleaved composites for excellent Mode I and Mode II delamination resistance. Compos Sci Technol 2019;175:143–50.
- [3] Kaynan O, Atescan Y, Ozden-Yenigun E, Cebeci H. Mixed Mode delamination in carbon nanotube/nanofiber interlayered composites. Compos Part B Eng 2018;154: 186–94. https://doi.org/10.1016/j.compositesb.2018.07.032.
- [4] Bilisik K, Erdogan G, Sapanci E, Gungor S. Mode-II toughness of nanostitched carbon/epoxy multiwall carbon nanotubes prepreg composites: Experimental investigation by using end notched flexure. J Compos Mater 2019;53:4249–71. https://doi.org/10.1177/0021998319857462.
- [5] Bilisik K, Syduzzaman M. Carbon nanotubes in carbon/epoxy multiscale textile preform composites: a review. Polym Compos 2021;42:1670–97. https://doi.org/ 10.1002/pc.25955.
- [6] Koirala P, van de Werken N, Lu H, Baughman RH, Ovalle-Robles R, Tehrani M. Using ultra-thin interlaminar carbon nanotube sheets to enhance the mechanical and electrical properties of carbon fiber reinforced polymer composites. Compos Part B Eng 2021;216:108842. https://doi.org/10.1016/j.compositesb.2021.108842.
- [7] Drake DA, Sullivan RW, Lovejoy AE, Clay SB, Jegley DC. Influence of stitching on the out-of-plane behavior of composite materials – a mechanistic review. J Compos Mater 2021;55:3307–21. https://doi.org/10.1177/00219983211009290.
- [8] Kharratzadeh M, Shokrieh MM, Salamat-talab M. Effect of interface fiber angle on the mode I delamination growth of plain woven glass fiber-reinforced composites. Theor Appl Fract Mech 2018;98:1–12. https://doi.org/10.1016/j. tafmec.2018.09.006.

- [9] Knopp A, Funck E, Holtz A, Scharr G. Delamination and compression-after-impact properties of z-pinned composite laminates reinforced with circumferentially notched z-pins. Compos Struct 2022;285:115188. https://doi.org/10.1016/j. compstruct 2022 115188
- [10] Ning N, Wang M, Zhou G, Qiu Y, Wei Y. Effect of polymer nanoparticle morphology on fracture toughness enhancement of carbon fiber reinforced epoxy composites. Compos Part B Eng 2022;234:109749. https://doi.org/10.1016/j. compositesb.2022.109749.
- [11] Tsang WL, Taylor AC. Fracture and toughening mechanisms of silica- and core-shell rubber-toughened epoxy at ambient and low temperature. J Mater Sci 2019;54:13938–58. https://doi.org/10.1007/s10853-019-03893-y.
- [12] Saravanakumar K, Arumugam V, Souhith R, Santulli C. Influence of Milled Glass Fiber Fillers on Mode I & Mode II Interlaminar Fracture Toughness of Epoxy Resin for Fabrication of Glass/Epoxy Composites. Fibers 2020;8. Doi: 10.3390/ fib8060036.
- [13] Vedrtnam A, Sharma SP. Study on the performance of different nano-species used for surface modification of carbon fiber for interface strengthening. Compos Part A Appl Sci Manuf 2019;125:105509. https://doi.org/10.1016/j. compositesa.2019.105509.
- [14] Fallahi H, Taheri-Behrooz F. Phenomenological constitutive modeling of the non-linear loading-unloading response of UD fiber-reinforced polymers. Composite Structures 2022;292:115671.
- [15] Vautard F, Fioux P, Vidal L, Schultz J, Nardin M, Defoort B. Influence of the carbon fiber surface properties on interfacial adhesion in carbon fiber–acrylate composites cured by electron beam. Compos Part A Appl Sci Manuf 2011;42:859–67. https:// doi.org/10.1016/j.compositesa.2011.03.015.
- [16] Yekani Fard M, Raji B, Pankretz H. Correlation of nanoscale interface debonding and multimode fracture in polymer carbon composites with long-term hygrothermal effects. Mech Mater 2020;150:103601. https://doi.org/10.1016/j. mechmat.2020.103601.
- [17] Wu Q, Zhao R, Xi T, Yang X, Zhu J. Comparative study on effects of epoxy sizing involving ZrO2 and GO on interfacial shear strength of carbon fiber/epoxy composites through one and two steps dipping routes. Compos Part A Appl Sci Manuf 2020;134:105909. https://doi.org/10.1016/j.compositesa.2020.105909.
- [18] Liu Yu, He D, Hamon A-L, Fan B, Haghi-Ashtiani P, Reiss T, et al. Comparison of different surface treatments of carbon fibers used as reinforcements in epoxy composites: Interfacial strength measurements by in-situ scanning electron microscope tensile tests. Compos Sci Technol 2018;167:331–8.
- [19] Yi C, Bagchi S, Dmuchowski CM, Gou F, Chen X, Park C, et al. Direct nanomechanical characterization of carbon nanotubes - titanium interfaces. Carbon N Y 2018;132:548–55.
- [20] Reale Batista MD, Drzal LT. Carbon fiber/epoxy matrix composite interphases modified with cellulose nanocrystals. Compos Sci Technol 2018;164:274–81. https://doi.org/10.1016/j.compscitech.2018.05.010.
- [21] Asadi A, Miller M, Moon RJ, Kalaitzidou K. Improving the interfacial and mechanical properties of short glass fiber/epoxy composites by coating the glass fibers with cellulose nanocrystals. Express Polym Lett 2016;10(7):587–97.
- [22] Fallahi H, Taheri-Behrooz F, Asadi A. Nonlinear mechanical response of polymer matrix composites: a review. Polym Rev 2020;60(1):42–85.
- [23] Gao S-L, Kim J-K. Cooling rate influences in carbon fibre/PEEK composites. Part 1. Crystallinity and interface adhesion. Compos Part A Appl Sci Manuf 2000;31: 517–30. https://doi.org/10.1016/S1359-835X(00)00009-9.
- [24] Kamae T, Drzal LT. Carbon fiber/epoxy composite property enhancement through incorporation of carbon nanotubes at the fiber-matrix interphase – Part II: Mechanical and electrical properties of carbon nanotube coated carbon fiber composites. Compos Part A Appl Sci Manuf 2022;160:107023. https://doi.org/ 10.1016/j.compositesa.2022.107023.
- [25] Semitekolos D, Trompeta A-F, Husarova I, Man'ko T, Potapov A, Romenskaya O, et al. Comparative physical-mechanical properties assessment of tailored surface-treated carbon fibres. Materials (Basel) 2020;13(14):3136.
- [26] Bilisik K, Sapanci E. Experimental determination of fracture toughness properties of nanostitched and nanoprepreg carbon/epoxy composites. Eng Fract Mech 2018; 189:293–306. https://doi.org/10.1016/j.engfracmech.2017.11.033.
- [27] Johnson AC, Hayes SA, Jones FR. The role of matrix cracks and fibre/matrix debonding on the stress transfer between fibre and matrix in a single fibre fragmentation test. Compos Part A Appl Sci Manuf 2012;43:65–72. https://doi. org/10.1016/j.compositesa.2011.09.005.
- [28] Zheng H, Zhang W, Li B, Zhu J, Wang C, Song G, et al. Recent advances of interphases in carbon fiber-reinforced polymer composites: a review. Compos Part B Eng 2022;233:109639.
- [29] Gangineni PK, Yandrapu S, Ghosh SK, Anand A, Prusty RK, Ray BC. Mechanical behavior of Graphene decorated carbon fiber reinforced polymer composites: an assessment of the influence of functional groups. Compos Part A Appl Sci Manuf 2019;122:36–44. https://doi.org/10.1016/j.compositesa.2019.04.017.
- [30] Kaynan O, Pérez LM, Asadi A. Cellulose nanocrystal-enabled tailoring of the interface in carbon nanotube- and graphene nanoplatelet-carbon fiber polymer composites: implications for structural applications. ACS Appl Nano Mater 2022;5: 1284–95. https://doi.org/10.1021/acsanm.1c03860.
- [31] Zhang RL, Gao B, Ma QH, Zhang J, Cui HZ, Liu L. Directly grafting graphene oxide onto carbon fiber and the effect on the mechanical properties of carbon fiber composites. Mater Des 2016;93:364–9. https://doi.org/10.1016/j. matdes.2016.01.003.
- [32] Ma K, Wang B, Chen P, Zhou X. Plasma treatment of carbon fibers: non-equilibrium dynamic adsorption and its effect on the mechanical properties of RTM fabricated composites. Appl Surf Sci 2011;257:3824–30. https://doi.org/10.1016/j. apsusc.2010.12.074.

- [33] Rong H, Dahmen K-H, Garmestani H, Yu M, Jacob KI. Comparison of chemical vapor deposition and chemical grafting for improving the mechanical properties of carbon fiber/epoxy composites with multi-wall carbon nanotubes. J Mater Sci 2013;48:4834–42. https://doi.org/10.1007/s10853-012-7119-2.
- [34] Li L, Liu W, Yang F, Jiao W, Hao L, Wang R. Interfacial reinforcement of hybrid composite by electrophoretic deposition for vertically aligned carbon nanotubes on carbon fiber. Compos Sci Technol 2020;187:107946. https://doi.org/10.1016/j. compscitech.2019.107946.
- [35] Tardy BL, Mattos BD, Otoni CG, Beaumont M, Majoinen J, Kämäräinen T, et al. Deconstruction and reassembly of renewable polymers and biocolloids into next generation structured materials. Chem Rev 2021;121(22):14088–188.
- [36] Kontturi E, Laaksonen P, Linder MB, Nonappa, Gröschel AH, Rojas OJ, et al. Advanced materials through assembly of nanocelluloses. Adv Mater 2018;30(24): 1703779
- [37] de Assis CA, Houtman C, Phillips R, Bilek EM (Ted), Rojas OJ, Pal L, et al. Conversion Economics of Forest Biomaterials: Risk and Financial Analysis of CNC Manufacturing. Biofuels, Bioprod Biorefining 2017;11:682–700. Doi: 10.1002/bbb.1782.
- [38] Zhang T, Cheng Q, Xu Z, Jiang B, Wang C, Huang Y. Improved interfacial property of carbon fiber composites with carbon nanotube and graphene oxide as multiscale synergetic reinforcements. Compos Part A Appl Sci Manuf 2019;125:105573. https://doi.org/10.1016/j.compositesa.2019.105573.
- [39] Mirjalili V, Hubert P. Modelling of the carbon nanotube bridging effect on the toughening of polymers and experimental verification. Compos Sci Technol 2010; 70:1537–43. https://doi.org/10.1016/j.compscitech.2010.05.016.
- [40] Chen J, Yan L, Song W, Xu D. Interfacial characteristics of carbon nanotubepolymer composites: a review. Compos Part A Appl Sci Manuf 2018;114:149–69. https://doi.org/10.1016/j.compositesa.2018.08.021.
- [41] Ou Y, González C, Vilatela JJ. Interlaminar toughening in structural carbon fiber/epoxy composites interleaved with carbon nanotube veils. Compos Part A Appl Sci Manuf 2019;124:105477. https://doi.org/10.1016/j.compositesa.2019.105477.
- [42] Mirjalili V, Yourdkhani M, Hubert P. Dispersion stability in carbon nanotube modified polymers and its effect on the fracture toughness. Nanotechnology 2012; 23(31):315701.
- [43] Feng WW, Reifsnider KL, Sendeckyj GP, Chiao TT, Steve Johnson W, Rodericks GL, et al. Composite interlaminar fracture: effect of matrix fracture energy. J Compos Tech Res 1984;6(4):176.
- [44] Bradley WL. Understanding the translation of neat resin toughness into delamination toughness in composites. Key Eng Mater 1989;37:161–98. https:// doi.org/10.4028/www.scientific.net/KEM.37.161.
- [45] Dadfar MR, Ghadami F. Effect of rubber modification on fracture toughness properties of glass reinforced hot cured epoxy composites. Mater Des 2013;47: 16–20. https://doi.org/10.1016/j.matdes.2012.12.035.
- [46] Khan SU, Kim J-K. Impact and delamination failure of multiscale carbon nanotubefiber reinforced polymer composites: a review. Int J Aeronaut Sp Sci 2011;12(2):
- [47] Adak NC, Chhetri S, Kuila T, Murmu NC, Samanta P, Lee JH. Effects of hydrazine reduced graphene oxide on the inter-laminar fracture toughness of woven carbon fiber/epoxy composite. Compos Part B Eng 2018;149:22–30. https://doi.org/ 10.1016/j.compositesb.2018.05.009.
- [48] Zakaria MR, Md Akil H, Abdul Kudus MH, Ullah F, Javed F, Nosbi N. Hybrid carbon fiber-carbon nanotubes reinforced polymer composites: a review. Compos Part B Eng 2019;176:107313. https://doi.org/10.1016/j.compositesb.2019.107313.
 [49] Sun L, Warren GL, O'Reilly JY, Everett WN, Lee SM, Davis D, et al. Mechanical
- [49] Sun L, Warren GL, O Reiny JY, Everett WN, Lee SM, Davis D, et al. Mechanical properties of surface-functionalized SWCNT/epoxy composites. Carbon N Y 2008; 46(2):320–8.
- [50] Vaisman L, Wagner HD, Marom G. The role of surfactants in dispersion of carbon nanotubes. Adv Colloid Interface Sci 2006;128–130:37–46. https://doi.org/ 10.1016/j.cis.2006.11.007.
- [51] Liu J, Suh H, Jee H, Xu J, Nezhad EZ, Choi C-S, et al. Synergistic effect of carbon nanotube/TiO2 nanotube multi-scale reinforcement on the mechanical properties and hydration process of portland cement paste. Constr Build Mater 2021;293: 123447.
- [52] Wang E, Dong Y, Islam MDZ, Yu L, Liu F, Chen S, et al. Effect of graphene oxidecarbon nanotube hybrid filler on the mechanical property and thermal response speed of shape memory epoxy composites. Compos Sci Technol 2019;169:209–16.
- [53] Bagotia N, Choudhary V, Sharma DK. Synergistic effect of graphene/multiwalled carbon nanotube hybrid fillers on mechanical, electrical and EMI shielding properties of polycarbonate/ethylene methyl acrylate nanocomposites. Compos Part B Eng 2019;159:378–88. https://doi.org/10.1016/j. compositesb.2018.10.009.
- [54] Basheer BV, George JJ, Siengchin S, Parameswaranpillai J. Polymer grafted carbon nanotubes—Synthesis, properties, and applications: a review. Nano-Struct Nano-Objects 2020;22:100429. https://doi.org/10.1016/j.nanoso.2020.100429.
 [55] Shariatnia S, Kumar AV, Kaynan O, Asadi A. Hybrid cellulose nanocrystal-bonded
- [55] Shariatnia S, Kumar AV, Kaynan O, Asadi A. Hybrid cellulose nanocrystal-bonded carbon nanotubes/carbon fiber polymer composites for structural applications. ACS Appl Nano Mater 2020;3:5421–36. https://doi.org/10.1021/ acsany 0c00755
- [56] Mariano M, El Kissi N, Dufresne A. Cellulose nanocrystals and related nanocomposites: Review of some properties and challenges. J Polym Sci Part B Polym Phys 2014;52:791–806. https://doi.org/10.1002/polb.23490.
- [57] Aramfard M, Kaynan O, Hosseini E, Zakertabrizi M, Pérez LM, Asadi A. Aqueous dispersion of carbon nanomaterials with cellulose nanocrystals: an investigation of molecular interactions. Small 2022;18:2202216. https://doi.org/10.1002/ smll.202202216.

- [58] Drescher P, Thomas M, Borris J, Riedel U, Arlt C. Strengthening fibre/matrix interphase by fibre surface modification and nanoparticle incorporation into the matrix. Compos Sci Technol 2013;74:60–6. https://doi.org/10.1016/j. compscitech.2012.10.004.
- [59] Monticeli FM, Ornaghi HL, Cioffi MOH, Voorwald HJC. The influence of carbon/glass/epoxy hybrid interfacial adhesion on the mode II delamination fracture toughness. Mech Compos Mater 2022;58(2):237–48.
- [60] Gibhardt D, Doblies A, Meyer L, Fiedler B. Effects of hygrothermal ageing on the interphase, fatigue, and mechanical properties of glass fibre reinforced epoxy. Fibers 2019;7(6):55.
- [61] Totry E, Molina-Aldareguía JM, González C, LLorca J. Effect of fiber, matrix and interface properties on the in-plane shear deformation of carbon-fiber reinforced composites. Compos Sci Technol 2010;70:970–80. https://doi.org/10.1016/j. compscitech.2010.02.014.
- [62] Katafiasz TJ, Greenhalgh ES, Allegri G, Pinho ST, Robinson P. The influence of temperature and moisture on the mode I fracture toughness and associated fracture morphology of a highly toughened aerospace CFRP. Compos Part A Appl Sci Manuf 2021;142:106241. https://doi.org/10.1016/j.compositesa.2020.106241.
- [63] Kaynan, O., Fallahi, H., Jarrahbashi, D., Asadi, A., 2022. September. In-Situ Bending Performance of Nanostructured Carbon Fiber Reinforced Polymer Composites. In Proceedings Of The American Society for Composites-Thirty-Seventh Technical Conference.
- [64] Tang Y, Yang H, Vignolini S. Recent progress in production methods for cellulose nanocrystals: leading to more sustainable processes. Adv Sustain Syst 2022;6: 2100100. https://doi.org/10.1002/adsu.202100100.
- [65] Gençer A, Schütz C, Thielemans W. Influence of the particle concentration and marangoni flow on the formation of cellulose nanocrystal films. Langmuir 2017;33: 228–34. https://doi.org/10.1021/acs.langmuir.6b03724.
- [66] Peng Y, Via B. The effect of cellulose nanocrystal suspension treatment on suspension viscosity and casted film property. Polymers (Basel) 2021;13(13):2168.
- [67] Oliveux G, Dandy LO, Leeke GA. Current status of recycling of fibre reinforced polymers: Review of technologies, reuse and resulting properties. Prog Mater Sci 2015;72:61–99. https://doi.org/10.1016/j.pmatsci.2015.01.004.

- [68] Standard test method for mode I interlaminar fracture toughness of unidirectional fiber-reinforced polymer matrix composites ASTM D 5528-01. Philadelphia (PA): American Society for Testing and Materials: 2001.
- [69] Standard test method for determination of the Mode II interlaminar fracture toughness of unidirectional fiber-reinforced polymer matrix composites D7905/ D7905M-14. West Conshohocken, PA: 2014.
- [70] Kelly A, Tyson WR. Tensile properties of fibre-reinforced metals: copper/tungsten and copper/molybdenum. J Mech Phys Solids 1965;13:329–50. https://doi.org/ 10.1016/0022-5096(65)90035-9.
- [71] Ansari F, Lindh EL, Furo I, Johansson MKG, Berglund LA. Interface tailoring through covalent hydroxyl-epoxy bonds improves hygromechanical stability in nanocellulose materials. Compos Sci Technol 2016;134:175–83. https://doi.org/ 10.1016/j.compscitech.2016.08.002.
- [72] Erden S, Ho KKC, Lamoriniere S, Lee AF, Yildiz H, Bismarck A. Continuous atmospheric plasma oxidation of carbon fibres: influence on the fibre surface and bulk properties and adhesion to polyamide 12. Plasma Chem Plasma Process 2010; 30:471–87. https://doi.org/10.1007/s11090-010-9227-6.
- [73] Guo CC, Zhao Y, Chen D, Zhan MS. Effect of sizing agent on interfacial shear strength of carbon fibre composites. Mater Res Innov 2014;18(sup4).
- [74] Quan D, Alderliesten R, Dransfeld C, Murphy N, Ivanković A, Benedictus R. Enhancing the fracture toughness of carbon fibre/epoxy composites by interleaving hybrid meltable/non-meltable thermoplastic veils. Compos Struct 2020;252: 112699. https://doi.org/10.1016/j.compstruct.2020.112699.
- [75] Cheng C, Chen Z, Huang Z, Zhang C, Tusiime R, Zhou J, et al. Simultaneously improving mode I and mode II fracture toughness of the carbon fiber/epoxy composite laminates via interleaved with uniformly aligned PES fiber webs. Compos Part A Appl Sci Manuf 2020;129:105696.
- [76] Hamer S, Leibovich H, Green A, Avrahami R, Zussman E, Siegmann A, et al. Mode I and Mode II fracture energy of MWCNT reinforced nanofibrilmats interleaved carbon/epoxy laminates. Compos Sci Technol 2014;90:48–56.
- [77] Vojtek T, Hrstka M. How to get a correct estimate of the plastic zone size for shear-mode fatigue cracks? Theor Appl Fract Mech 2019;104:102332. https://doi.org/10.1016/j.tafmec.2019.102332.